Indian J. Phys. **73A** (5), 717–723 (1999)

NOTE

IJP A
— an international journal

Band structure calculation of momentum density in ruthenium

S B Shrivastava and S K Shastri
School of Studies in Physics, Vikram University,
Ujjain-456 010, India

Received 2 December 1998, accepted 24 March 1999

Abstract : Band structure calculation of two photon momentum density distribution (TPMD), the angular correlations for positron annihilation radiations (ACAR) and the Compton profile (CP) have been performed in the *fcc* structure of the 4*d* transition metal ruthenium. The calculated results have been plotted along the three directions of high symmetry and discussed in terms of the observed energy band structure Strong discontinuities in the TPMD have been observed along the [100] direction at $p = 4.8$ mrad and along [111] direction at $p = 3.7$ mrad A comparison of ACAR in Ru has been made with that in Rh It has been observed that the ACAR in Ru gives a much broader distribution as compared to that in Rh.

Keywords : Band structure of Ru, electron states, positron annihilation

PACS Nos. : 71 10 -w, 71 60 +z, 78 70 Bj

The electronic structure of 4*d* metals is of particular interest due to the unfilled *d* states and their peculiar properties. In these metal the Fermi level intersects the *d* bands leading to a complex Fermi surface topology. The strong *p* dependence of the momentum density distributions corresponding to various Fermi surface sheets combined with the existence of important Umklapp components, severely complicates the interpretation of experimental data. The only way to understand the electronic structure of these metals is to perform a detailed band structure calculation of electron momentum densities (EMD). Such calculations also provide a basis to u derstand the results of angular correlation for positron annihilation radiations and the Compton profile studies in these metals [1]. EMD calculations have been reported in many of the 4*d* metals by a number of authors [2–5]. However, no theoretical calculation of EMD has been done so far in ruthenium. The only Fermi surface study reported was by Coleridge [6], for the De-Hass van Alphen oscillations. The result was interpreted on the basis of a rigid band model and using the

band structure of Re. Recently, Sharma *et al* [7] have performed an experimental study of Compton profile in *hcp* Ru. However, they have given only the difference between experimental and theoretical results. In the present work, we report the results of our calculations of the energy band structure, the positron wave function, the two photon momentum density (TPMD), the angular correlations for positron annihilation (ACAR) and the Compton profile (CP) in *fcc* ruthenium. The aim is to understand the EMD in Ru and to compare the results with those in Rh so as to understand the effect of change in *d* band on EMD and ACAR.

The momentum density distribution of the photon pairs (TPMD) from the annihilation of thermalised positrons with electrons of wave vector $\boldsymbol{k}$ in the j-th energy band is given by [1]

$$\rho(\boldsymbol{P}) = \Sigma_{K,j} f(\boldsymbol{k}, j) \left| A_j(\boldsymbol{k}, \boldsymbol{p})^2 \delta(\boldsymbol{p} - \boldsymbol{k} - \boldsymbol{K}_i) \right|^2, \tag{1}$$

where $f(\boldsymbol{k}, j)$ describes the occupation of the electron state $\psi_{k,j}$ having wave vector $\boldsymbol{k}$ and band index j, $A_j(\boldsymbol{k}, \boldsymbol{p})$ is the overlap matrix element and $\boldsymbol{K}_j$ is the reciprocal lattice vector responsible for the Umklapp process. The overlap matrix element is related to the electron wave function $\psi_{k,j}(\boldsymbol{r})$ and the wave function of the thermalised positron $\psi_+(\boldsymbol{r})$ in the ground state ($\boldsymbol{k} = 0$) through the relation

$$A_j(\boldsymbol{k}, \boldsymbol{p}) = \int_{\text{cell}} \exp(-i\boldsymbol{p}.\boldsymbol{r}) \psi_{k,j}(\boldsymbol{r}) \psi_+(\boldsymbol{r}) d\boldsymbol{r}. \tag{2}$$

Eq. (1) also represents the electron momentum density derived from Compton scattering (EMD) if $\psi_+(\boldsymbol{r})$ in eq. (2) is replaced by unity. The calculation of $\rho(\boldsymbol{p})$ from equation (1) requires the computation of the energy band structure the electron wave function $\psi_{k,j}(\boldsymbol{r})$ and the positron wave function. In the present work, the calculation of energy band structure and electron wave function has been performed employing the approximate technique of band structure calculation of Hubbard [8] and as developed by Mijnarends [9]. The crystal potential employed in the numerical calculation is the Muffin-tin potential as given by Moruzzi *et al* [10]. In this the charge densities were spherically sysmmetric inside, touching, but non-overlapping, spheres and constant in the region between the spheres. Moruzzi *et al* [10] had chosen the reference energy such that the potentials as zero in the interstitial region. These potentials are interpolated on a Hermann-skillman mesh. In the calculation of energy eigen values partial waves up to $\lambda_{\max} = 3$ were used in the expansion of wave function inside the inscribed sphere while 137 reciprocal lattice vectors including 15 in the preferred set were used in the expansion of the wave function outside the inscribed sphere.

The positron is known to be thermalised before annihilation and is, therefore, assumed to be in the ground state ($\boldsymbol{k} = 0$). The positron wave function is periodic according

to Bloch theorem and may be expanded as a Fourier series in terms of the reciprocal lattice vectors following Gould *et al* [11]

$$\psi_+(r) = 1/(\tau)^{1/2} \sum_K A_K \exp(iK.r) \tag{3}$$

is written in symmetrized form and solved easily using the Fourier coefficient.

$$V_{K-K'} = (1/\tau)V(r)\exp[i(K-K')r]dr \tag{4}$$

The first coefficient was adjusted so that $\psi_+(r=0) = \tau^{-1/2}\sum_K A_K = 0$ subject to the normalization condition $\sum_K |A_K|^2 = 1$. The potential $V(r)$ in which the positron moves is assumed to be the electrostatic potential used in the calculation of the electronic wave function. Thus, no correlation between electron and the positron is taken into account. The first ten shells (ten representative vectors of the shells) and 137 plane waves in the expansion of the *fcc* structure were included in the calculations of $\psi_+(r)$. The band profile for the long slit geometry angular correlation has been obtained from

$$N(P_z) = \int_p^\infty \rho_{sph}(p)p\,dp \tag{5}$$

where the spherically averaged $\rho_{sph}(P)$ was obtained averaging ρ_{100}, ρ_{110} and ρ_{111} according to Betts *et al* [12].

$$\rho_{sph}(p) = (1/35)[10\rho_{100}(p) + 16\rho_{110}(p) + 9\rho_{111}(p)] \tag{6}$$

The band profile for Compton scattering $J(P_z)$ has been obtained using eq. (6) but by taking $\rho_{sph}(P)$ pertaining to EMD *i.e.* without the positron wave function.

The energy band structure as obtained from the present calculation are shown in Figure 1 along some important symmetry directions. The Fermi energy is shown by dotted

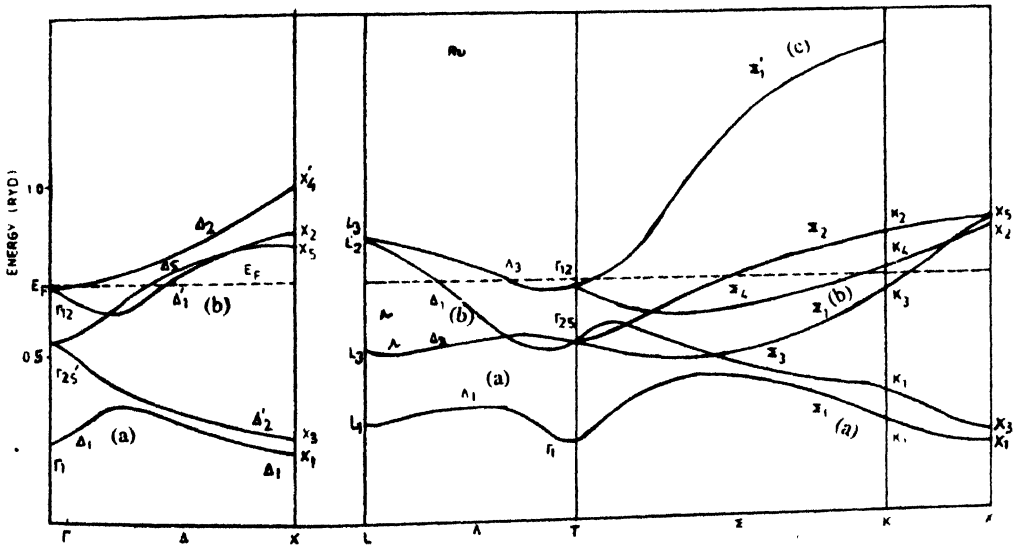

Figure 1. Energy bands for Ru along some symmetry directions.

lines. A look at the band structure (Figure 1) shows that along Δ direction the $\Delta_1(a)$ band lies well below the Fermi level and the $\Delta_1(b)$ band crosses the Fermi level. Along Σ direction the $\Sigma_1(c)$ band lies above the Fermi level while $\Sigma_1(a)$ and $\Sigma_1(b)$ bands are below the Fermi level. Along Λ direction $\Lambda_1(a)$ band lies below the Fermi level while $\Lambda_1(b)$ band crosses the Fermi level. These features have been found to give prominent contribution to corresponding momentum density distributions as discussed in Section 4.

The results of the two photon momentum density distributions (TPMD) in *fcc* Ru as obtained from the present calculations for 4*d* and conduction electrons are plotted in Figure 2 along the three symmetry directions [100], [110] and [111]. According to a selection rule pointed out by Mijnarends [9] only the respective bands Δ_1, Σ_1, Λ_1 belonging

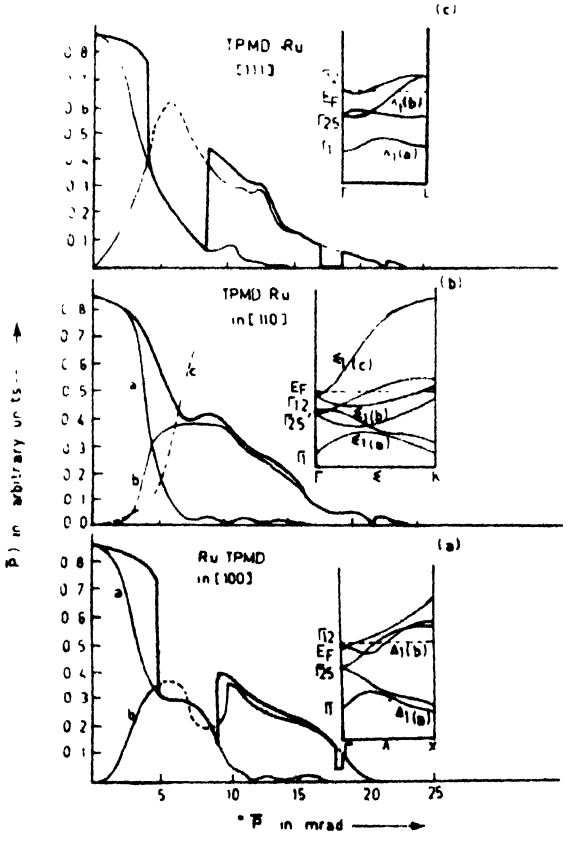

Figure 2. Calculated two photon momentum density distribution in Ru along (a) [100], (b) [110] and (c) [111] directions

to the totally symmetric irreducible representation can contribute to the total TPMD in the first Brillioulin zone. The contribution to total TPMD from the individual bands is also shown in above figure. The TPMD along [100] direction shows significant structures between $p \approx 4.8$ to 9 mrad. The band structure along this direction shows that the $\Delta_1(a)$ band lies well below the Fermi level and is fully occupied. Hence, this band contributes

fully to the total TPMD and gives *s*-like contribution at low momenta. However, the $\Delta_1(b)$ band is partially occupied and crosses the Fermi level. This gives rise to a strong discontinuity in the total TPMD at $p \approx 4.8$ mrad. This is because of the unoccupied part of the $\Delta_1(b)$ band shown by the dotted line. The contribution due to the $\Delta_1(b)$ band rises steeply at low momenta due to the *s-d* hybridization. As a result of this hybridization the upper band contributes mainly as *s*-character near the Fermi energy. From the position of the discontinuity, the Fermi momenta can be determined. The effect of Umklapp processes has been observed in the higher zones, thus, giving a peak at $p = 18$ mrad.

Along [110] direction, both the $\Sigma_1(a)$ and $\Sigma_1(b)$ bands lie much below the Fermi level and are fully occupied while the $\Sigma_1(c)$ band lies above the Fermi level and is unoccupied. Thus, the total TPMD is a sum of the contributions from the two bands in the first Brillouin zone. The contribution from the $\Sigma_1(a)$ band falls rapidly at low momenta and is mainly due to *s-p* character. With the increase in *k*-values the wave fucntion hybridizes with the *d* bands. The contribution from the *d* bands increases and give a large contribution to the total TPMD for p between 4 to 13 mrad. Thus, giving a broad distribution to the total TPMD. The contribution of this band is *d*-like throughout the Brillouin zone. No discontinuity in the first Brillouin zone could be observed along this direction. The effect of Umklapp processes has been observed in the higher zone.

A prominent feature along [111] direction is the occurrence of a strong discontinuity at $p \approx 3.7$ mrad arising from the crossing of the $\Lambda_1(b)$ band with the Fermi level in the first *B*-zone. The total TPMD shows a strong dip between $p \approx 3.7$ to 8.3 mrad and a strong step at $p \approx 8.3$ mrad. The contribution from $\Lambda_1(b)$ band rises rapidly and becomes unoccupied at $p \approx 3.7$ mrad. The contribution from $\Lambda_1(a)$ band is more or less similar in nature to that along other directions. A broader contribution to the total TPMD has been observed for p between 8.3 to 14.7 mrad along this direction. The effect of *U*-processes has been observed in the form of a small discontinuity at $p = 16.5$ mrad and a step at $p = 21.3$ mrad.

Besides the calculation of TPMD, we have also performed the computation of EMD pertaining to Compton profile in ruthenium. The EMD for 4*d* and conduction electrons in

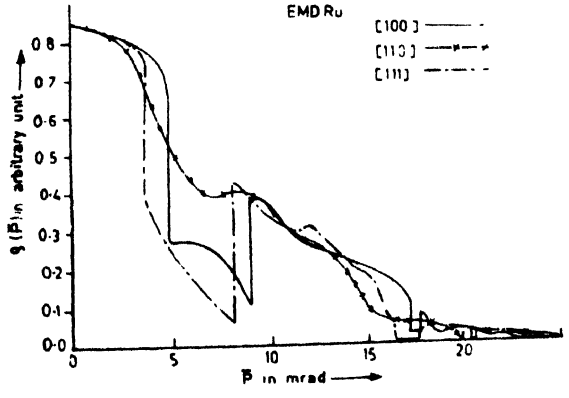

Figure 3. Calculated momentum density in fcc Ru along [100], [110] and [111] directions.

ruthenium along the three symmetry directions are presented in Figure 3. Looking to these curves one observes that the nature of the TMPD and EMD are the same. The main difference occurs in the higher zones where the EMD curves give a larger contribution to $\rho(p)$. Thus the effect of the absence of Ψ_+ is found to be important in case of the high momentum region only. Along [100] direction the $\rho(p)$ extends up to $p \approx 23.5$ mrad, while the same in case of TPMD terminates at $p \approx 21$ mrad. Similar effects have been observed along other directions also.

The calculated band profile for ACAR ($N(p_z)$) and the band electron Compton profile ($J(p_z)$), are plotted in Figure 4 for the comparison of band ACAR and band CP. The curves are identical at low momenta *i.e.* up to $p \approx 6$ mrad. But the high momenta the $J(p_z)$ curve gives a higher and broader contribution. While the band ACAR curve ends at 20 mrad, the band CP curve extends up to 23.5 mrad. Thus, the amplitude of the Compton profile is higher at high p values. This is consistent as in case of the Compton profile the absence of positron wave function increases the contribution to the $\rho(p)$. In the same figure the band ACAR for Rh also has been plotted for comparison.

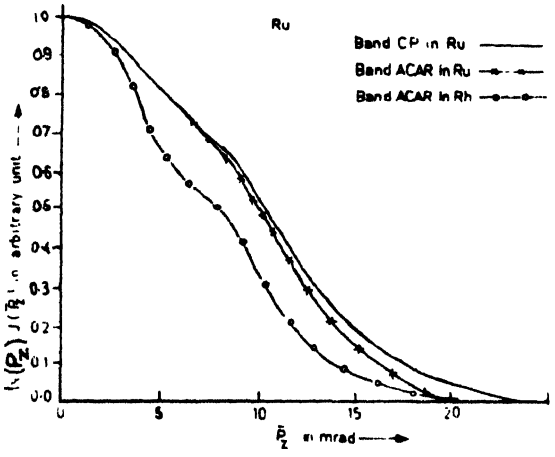

Figure 4. Comparison of the band CP $J(p_2)$ with ACAR (Np_2) in Ru. The band (ACAR) in Rh is also plotted for comparison.

The ACAR in Ru has been observed to be much broader as compared to in Rh. This could be due to large d band width in Ru, suggesting strong hybridization in case of Ru. Experimental studies of EMD in Ru are, however, needed to verify the above facts.

References

[1] P E Mijnarends in *Positron Solid State Physics* eds. W Brandt and A Dupasquier (Amsterdem : North Holland) (1983)

[2] A Kshirsagar, D G Kanhere and R M Singru in *Positron Annihilation* eds. L Dorikens-Vanpraet, M Dorikens and D Segers (Singapore : World Scientific) p 236 (1988)

[3] S B Shrivastava and H P Bonde *Phys. Stast. Sol. (b)* **139** 155 (1987)

[4] D G Kanhhere and R M Singru *Phys. Lett.* **53A** 67 (1975)

[5] S M Sharma, P Chidambaram and S K Sikka in *Positron Annihilation* eds. P C Jain, R M Singru and K P Gopinathan (Singapore : World Scientific) p 52 (1985)

[6] P T Coleridge *J. Low Temp. Phys.* **1** 1254 (1969)

[7] B K Sharma, R K Kothari, K B Joshi, M D Sharma and B L Ahuja *Solid State Phys.* (India) **37C** 108 (1994)

[8] J Hubbard *J. Phys.* **C2** 1222 (1969)

[9] P E Mijnarends *Physica* **63** 235 (1973)

[10] V L Moruzzi, J F Janak and A R Williams *Calculated Electronics Properties of Metals* (New York : Pergaman) (1978)

[11] A G Gould, R N West and B G Hogg *Can. J. Phys.* **50** 2294 (1972)

[12] D D Betts, A B Bhatia and M Wyman *Phys. Rev.* **104** 37 (1956)